Carbon Science

Vol. 1, No. 1 June 2000 pp. 36-40

Initial Electrochemical Insertion/Desertion of Lithium into Hard Carbon

Chil-Hoon Doh*, Seong-In Moon, Mun-Soo Yun, Chang-Soo Jin, Bong-Soo Jin and Seung-Wook Eom

Battery Research Group, Korea Electrotechnology Research Institute, Changwon 641-120, Korea

*e-mail: *chdoh@keri.re.kr*

(*Received 5 March 1999; accepted 5 June 1999*)

Abstract

The initial irreversible capacity (*IIC*) of a hard carbon during the charge/discharge reaction is strongly affected by both the initial irreversible capacity on the carbon surface (IIC_S) and the initial irreversible lithium insertion into carbon (IIC_B). The initial coulombic efficiency of the insertion and the desertion of lithium (*IIE*) can be used as a performance to classify IIC_B of the carbon. The IIC_B was proportional to the specific discharge capacity with a slope, $IIE^{-1} - 1$. The *IIE* of hard carbon had four regions. IIE_A for the region of 0~95 mAh/g of Q_{D1} was 60.2%. IIE_B and IIE_C for the regions of 95~172 mAh/g and 172~308 mAh/g had 84.9% and 91.5%, respectively. IIE_D was appeared above 308 mAh/g. But, the IIE_D was reduced to 82.1% compared with IIE_C. These *IIE* might be corresponding to lithium desertion from carbon at the region of 0~172 mAh/g range, lithium desertion from the micropore of carbon at the region of 172~308 mAh/g range, and to the lithium stripping of the plated lithium for the region above 308 mAh/g, respectively.

Keywords : *Initial Li^+ Intercalation, Hard Carbon, Intercalation Efficiency, Initial Irreversible Capacity of Surface & Bulk*

1. Introduction

Lithium ion cell [1, 2] is the outstanding battery system because of good performances such as high operating voltage, high energy density, long cycle life, no memory effect, and environmental compatibility.

The most promising lithium intercalation anode material is the layer structured carbon [3] although it has somewhat low specific capacity compared to that of lithium metal.

The use of an organic electrolyte causes the irreversible decomposition of organic molecules at the anode surface because of cathodic reaction with the resultant current loss. The decomposed materials [4-6] are gaseous products and insoluble salts that are deposited to the electrode surface.

Despite of the good cycle performance of the carbon, the initial irreversible capacity [7-11] of the carbon may affect material balancing of the cathode and the anode. Material balancing is related to the capacity and the cycle life.

The cathodic reaction of the carbon can be categorized to three: (i) the irreversible solvent decomposition at the carbon surface, (ii) the lithium intercalation into the carbon, and (iii) the lithium plating. The incomplete discharge of lithium leads the current loss, which mainly appeared at the first charge, and is called the initial irreversible capacity (*IIC*). The charge is occurred during potential decrease of the carbon electrode versus Li/Li^+ reference electrode. Generally, the *IIC* of the carbon anode is known as follows [8]: (i) the solvent decomposition at the carbon electrode surface, (ii) the irreversible reaction of the lithium with functional groups of carbon surface such as carboxyl, hydroxyl and carbon hydride [7], (iii) the irreversible insertions of the lithium into the bulk of carbon and (iv) the irreversible lithium plating/striping, which is not appear in the normal operation range. Therefore, *IIC* could be characterized as the summation of *IIC* of the surface reaction (IIC_S) and the bulk reaction (IIC_B) as shown equation (1). And, *IIC* is the difference between the first specific charge capacity (Q_{C1}) and the first specific discharge capacity (Q_{D1}). The irreversible solvent decomposition and the irreversible reaction of lithium with functional groups of carbon surface take place prior to the lithium intercalation [13, 14].

$$IIC = IIC_B + IIC_S = Q_{C1} - Q_{D1} \quad (1)$$

Dahn et al. [8] presented qualitative and quantitative analyses with the reaction of functional groups of carbon surface. The exposed carbon surface to the reactive gases such as steam, air and oxygen has the higher *IIC* than the pristine carbon. Matsumura et al. [9] also studied on the irreversible capacity of carbon by the potential step method. In the case of the ribbon-like carbon film, heat-treated at 1500ºC, the irreversible capacity between 0.25 V_{Li/Li^+} and 0.01 V_{Li/Li^+} is 66% of the total irreversible capacity. They confirmed also that the lithium content in the carbon material is 66% by the chemical analysis. They concluded that lithium remains on the surface and in the bulk of discharged carbon electrode.

In this study, we obtained the initial irreversible capacity (*IIC*) pattern as a function of the specific discharge capacity (Q_{D1}) through the test of electrochemical cells containing hard carbon. And the relationship between *IIC*, IIC_S, IIC_B, and *IIE* was discussed.

2. Experimental

2.1. Carbon

Structural characteristics of the hard carbon used was investigated. Lattice parameters were measured by XRD (APD 1700, Phillips Corp.) with the scan rate of 0.05 deg/sec. The d_{002} spacing of the hard carbon was 3.69 Å. The degree of graphitization was zero because the d_{002} spacing exceeds 3.44 Å [15]. The XRD pattern was shown in Fig. 1. The morphology of the hard carbon powder was observed with a scanning electron microscope (SEM; S-2700, Hitachi) and shown in Fig. 2.

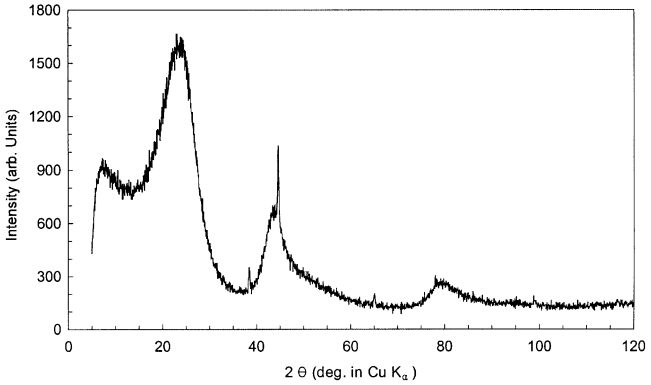

Fig. 1. XRD pattern of a hard carbon powder.

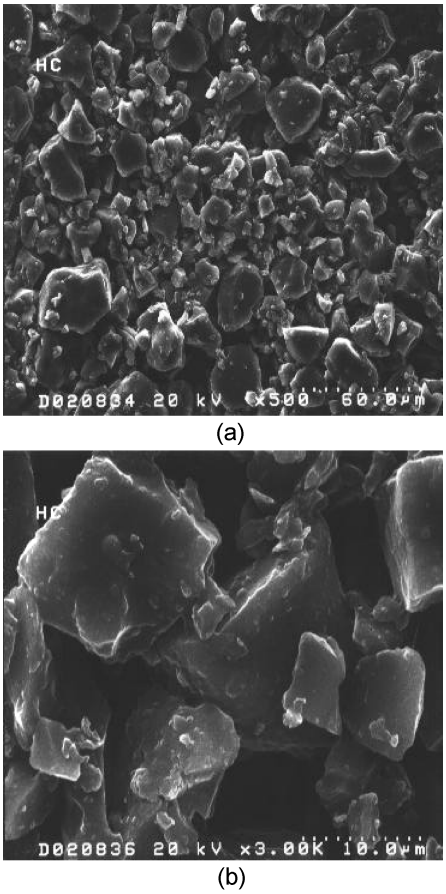

Fig. 2. SEM images of a hard carbon powder: (a) × 500 (b) × 2,000.

2.2. The Electrochemical Cell

Three-electrode-test-cells were constructed with a hard carbon [16]. The carbon electrodes (2 × 4 cm^2 on the single side of Cu foil) was made by the coating of the carbon powder slurry onto the copper foil current collector. Polyvinylidene fluoride (PVDF) and 2-methyl pyrrolidone (NMP) were used as a binder and a slurry solvent, respectively. The carbon electrodes contained 10 wt.% binder. The carbon electrodes were dried at 100°C and then calendered by the twin roll. The carbon electrodes had a coverage of ~4 mg/cm^2, excluding PVDF and the copper current collector. The apparent density of the carbon electrodes was 1.0 g/cm^3. The reference electrode used was lithium metal on a nickel tab. Lithium foil (2.5 × 4.5 cm^2) was used as counter electrode. A separator (Cellgard 2500, Hoechst) was sandwiched between the carbon electrode and the lithium counter electrode. The stack of the carbon electrode, separator, and lithium counter electrode was wound to make a jelly roll by the winding machine. The jelly rolls were dried under vacuum at room temperature for at least 12 hours. The test cell was constructed on Pyrex glass tube with jelly roll, the lithium reference electrode, and the electrolytic solution of 1 M $LiPF_6$ in a mixed propylene carbonate (PC) and diethyl carbonate (DEC) solvent (1 : 1 by volume) with (1PPDEC; battery-grade, Mitsubishi Petrochemical Co.).

2.3. Electrochemical Tests

Typical charge/discharge tests for the carbon electrodes were carried out using the galvanostatic technique with 2 mA/cell (0.25 mA/cm^2; ca. 10 hour rate) at 0 to 3 V vs. Li/Li^+ by using the Maccor series 2000 charge/discharge tester. One hour of the rest time was allowed between charge and discharge step. All experiments were carried out at 25°C in a dry argon atmosphere. A series of charge/discharge tests were performed by the variation of the first specific charge capacity (Q_{C1}) with each fresh cells.

3. Results and Discussion

A potential profile against the specific discharge capacity, and a differential-capacity profile against the potential were presented in Fig. 3 and Fig. 4, respectively. During the first charge, a potential plateau at 0.9 V_{Li/Li^+} was known as the irreversible reaction at the carbon surface [4, 5, 6]. The lithium intercalation into carbon proceeded to ca. 30 mV_{Li/Li^+}. And then the lithium insertion into the carbon including lithium plating proceeded from ca. 30 mV_{Li/Li^+} to –40 mV_{Li/Li^+}. During the first discharge in Fig. 3 and Fig. 4, the lithium desertion proceeded with four patterns. They were ~308 mAh/g (region D), 308~172 mAh/g (region C), 172~95 mAh/g (region B) and 95~0 mAh/g (region A) based on the reverse scale of the specific capacity starting from the end of discharge. The end potential of regions D, C, B, and A were

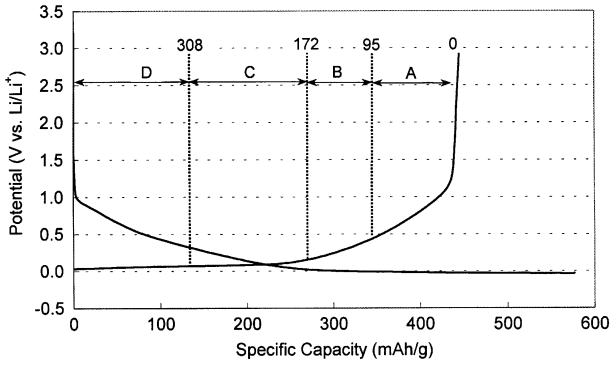

Fig. 3. A potential profile of a hard carbon/Li cell by the galvanostatic charge/discharge. carbon material; 33 mg, electrolyte; 1 M $LiPF_6$/EC + DEC (1 : 1 v/v) current density; 2 mA/cell, charge cut-off; 577 mAh/g-C, discharge cut-off; 3 V vs. Li/Li^+

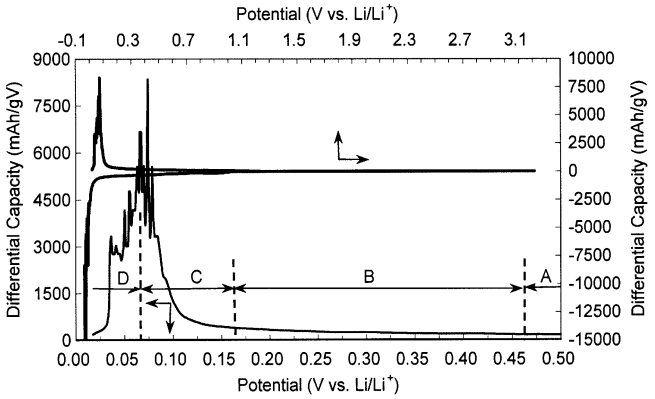

Fig. 4. A differential-capacity profile of a hard carbon/Li cell by the galvanostatic charge/discharge. carbon material; 33 mg, electrolyte; 1 M $LiPF_6$/EC + DEC (1 : 1 v/v) current density; 2 mA/cell, charge cut-off; 577 mAh/g-C, discharge cut-off; 3 V vs. Li/Li^+

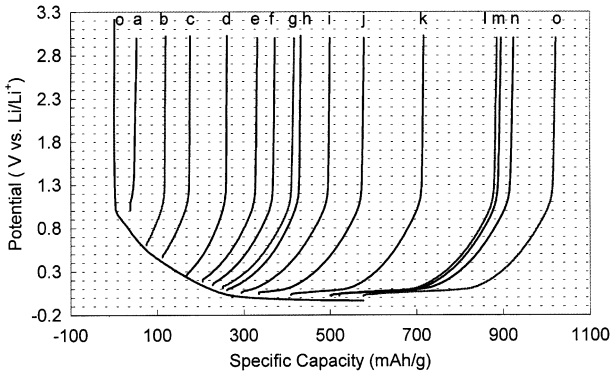

Fig. 5. Potential profiles of a hard carbon/Li cell as a function of the specific charge capacity by the galvanostatic charge/discharge. electrolyte; 1 M $LiPF_6$/EC + DEC (1 : 1 v/v), current density; 2 mA/cell charge cut-off; control of the Q_{C1}, discharge cut-off; 3 V vs. Li/Li^+

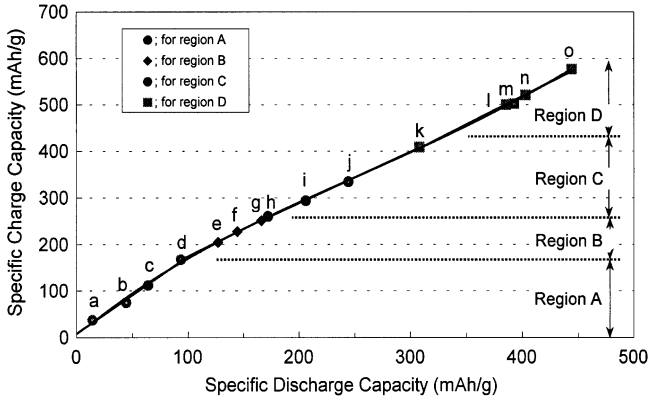

Fig. 6. The initial specific charge capacity as a function of the initial specific discharge capacity for a hard carbon/Li cell.

70 mV_{Li/Li^+}, 165 mV_{Li/Li^+}, 460 mV_{Li/Li^+}+ and 3,000 mV_{Li/Li^+}, respectively. The different slope was measured at each regions as depicted in Fig. 6.

To obtain the initial charge/discharge characteristics as a function of Q_{D1}, a series of tests were performed by controlling Q_{C1}. Fig. 5 presents a typical charge potential profile (o) until about 577 mAh/g-carbon and a series of discharge potential profiles (a~o). From these experiments, Q_{C1} and Q_{D1} were collected and plotted in Fig. 6 in four distinguishable linear region. Regions A and B may correspond to the lithium insertion/desertion. Region C corresponds to the lithium plating into the micropore (or cavity [17] and region D corresponds to the lithium plating on the carbon surface and into the macropore, respectively.

The fitted line at Fig. 6 have the relation of equations (2)~(5) to show that the discharge capacity is proportional to the charge capacity in the given region. This relation is shown in Fig. 7 and equation (6). The initial coulombic efficiency of the insertion and the desertion of lithium (*IIE*) is a parameter of the lithium insertion/desertion reversibility as shown in equation (8), which is a differential of equation (6). From equation (1) and (6), IIC_B is proportional to Q_{D1} as shown in equation (8). In the ideal electrode-electrolyte system, IIC_S is 0 mAh/g and *IIE* is 100%. A previous study on the *IIC* was performed with the graphite [18].

For region A; $Q_{C1} = Q_{D1}/0.602 + 7.8$ (2)

For region B; $Q_{C1} = Q_{D1}/0.849 + 56.8$ (3)

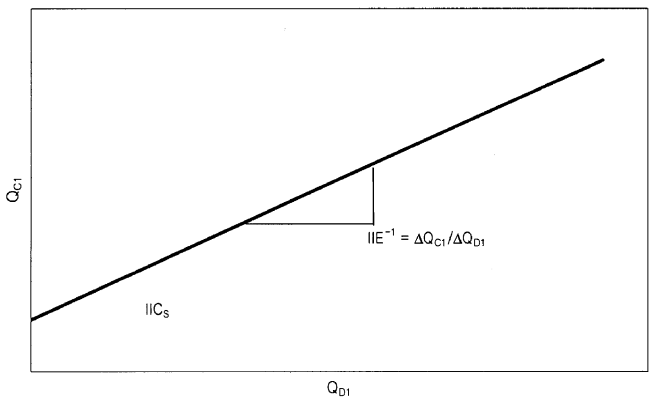

Fig. 7. Relation between the first specific charge and discharge capacity.

For region C; $Q_{C1} = Q_{D1}/0.915 + 70.3$ (4)

For region D; $Q_{C1} = Q_{D1}/0.821 + 30.5$ (5)

$Q_{C1} = IIE^{-1} * Q_{D1} + IIC_S$ (6)

$IIE = \Delta Q_{D1}/\Delta Q_{C1}$ (7)

$IIC_B = (IIE^{-1} - 1) * Q_{D1}$ (8)

Therefore, IIC_S and IIE for the region A were 7.81 mAh/g and 60.2%, respectively. IIE for regions B, C and D were also evaluated as 84.9%, 91.5% and 82.1%, respectively. Therefore, the reversibility of lithium was increased from region A to region C, but that was decreased for region D compared to region C. These IIE might be corresponding to the lithium desertion from the carbon matrix for a region of 0~172 mAh/g (Region A and B) and from the micropore of carbon for region of 172~308 mAh/g (Region C), and to the lithium stripping of the plated lithium for region above 308 mAh/g (Region D), respectively [19, 20, 21].

IIC could be written as from equation (9) to equation (12) through equations (1), (8) and (2-5), as shown in Fig. 8.

For region A; $IIC = 0.662Q_{D1} + 7.8$ (9)

For region B; $IIC = 0.178Q_{D1} + 56.8$ (10)

For region C; $IIC = 0.093Q_{D1} + 70.3$ (11)

For region D; $IIC = 0.218Q_{D1} + 30.5$ (12)

Equations (2)~(5) and (9)~(12) were summarized in Table 1.

A polynomial of IIC for all region was depicted using equation (13), as shown in Fig. 8 with dotted line. The equation (13) can be used for the design of the practical cell.

$$IIC = 5.45 + 0.888Q_{D1} - 0.0029Q_{D1}^2 + 3E-6Q_{D1}^3 + 2E-9Q_{D1}^4 \quad (13)$$

Jean et al. [22] showed that the IIC of a petroleum coke varies with the initial charge capacity. In Fig. 9, Jean's data (Fig. 1(b) in Reference 22) was redrawn as a function of the initial discharge capacity. The linear fit of Q_{C1} and IIC against Q_{D1} has good accordance. Therefore, we could evaluate the relationship of equation (14) and (15)

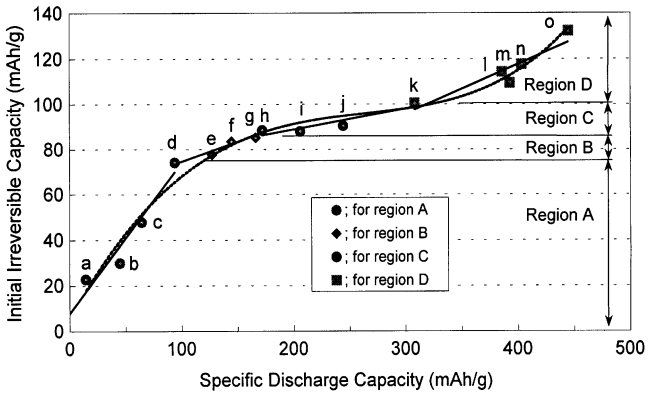

Fig. 8. The initial irreversible capacity as a function of the initial specific discharge capacity for a hard carbon/Li cells.

Table 1. IIE, $(IIE^{-1} - 1)$ and Intercepts of The Lithium Insertion/Desertion of Hard Carbon/1 M $LiPF_6$/EC + DEC (1 : 1)/Li Cell

Region		A	B	C	D
Range (mAh/g)	Dcharge	0~95	95~172	172~308	308~
	Charge	0~170	170~260	260~409	409~
IIE (%)		60.2	84.9	91.5	82.1
$(IIE^{-1} - 1)$		66.2	17.8	9.3	21.8
Intercept (mAh/g)		7.81	56.8	70.3	30.5

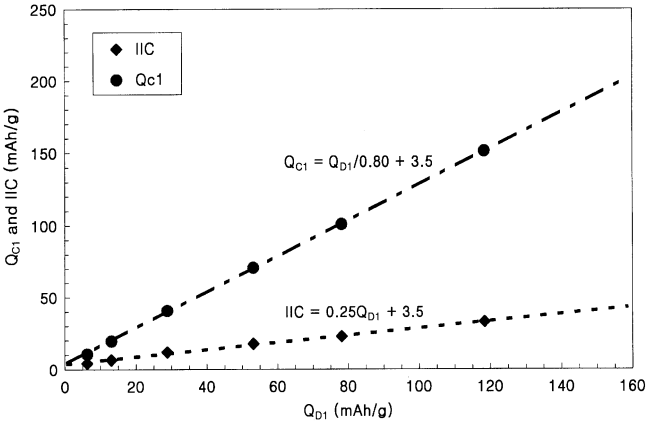

Fig. 9. The initial specific charge capacity and the initial irreversible capacity as a function of the initial specific discharge capacity for Fig. 1(b) of ref. no. 22.

$$Q_{C1} = \frac{Q_{D1}}{0.8} + 3.5 \quad (14)$$

$IIC = 0.25Q_{D1} + 3.5$ (15)

Equations (14) and (15) are the same format with equations (6), (1) and (8). For Jean's data, IIE and IIC_S are 80% and 3.5 mAh/g, respectively.

Through these results, IIC could be distinguished with IIC_S and IIC_B. IIC_B had a linear relationship with Q_{D1} having a slope $(IIE^{-1} - 1)$ as shown in equation (7). IIC_S and IIE can be used as the parameter to evaluate the characteristics of carbon anode and electrolyte.

4. Conclusions

The initial irreversible capacity of a hard carbon was distinguished with IIC_S (intercept of region A) and IICB. IICB had a linear relationship with a slope of $(IIE^{-1} - 1)$ as a function of Q_{D1}. IIE had different values caused by reaction mode between carbon and lithium ion.

$$IIC = IIC_B + IIC_S = (IIE^{-1} - 1)Q_{D1} + IIC_S = Q_{C1} - Q_{D1}$$

These IIE values are corresponding to the lithium desertion from the carbon for region of 0~172 mAh/g and from the micropore of carbon for region of 172~308 mAh/g, and to the lithium stripping of the plated lithium for the region

above 308 mAh/g, respectively. IIE_A for a region of 0~95 mAh/g of Q_{D1} was 60.2%. IIE_B and IIE_C for regions of 95~172 mAh/g and 172~308 mAh/g increased to 84.9% and 91.5%, respectively. IIE_D for region above 308 mAh/g decreased to 82.1% compared with IIE_C.

Acknowledgement

This work was performed under a Midterm-Technology Development Program, sponsored by the MOCIE of Korea and STC Corporation.

References

[1] Dahn, J. R.; Sleigh, A. K.; Shi, H.; Way, B. M.; Weydanz, W. J.; Reimers, J. N.; Zhong, Q.; Sacken, U. "*Lithium Batteries; New Materials, Developments and Perspectives*", ed. G. Pistoia, Elsevier, New York, 1994, 1.

[2] Goodenough, J. B. et al. "*Lithium Ion Batteries; Fundamentals and Performance*", ed. M. Wakihara; O. Yamamoto, Wiley-VCH, New York, 1998, 1.

[3] Dresselhaus, M. S.; Dresselhaus, G. *Adv. Phys.* **1981**, *30*, 139.

[4] Kanamura, K.; Tamura, H.; Shiraishi, S.; Takehara, Z. *J. Elecrochem. Soc.* **1995**, *142*, 340.

[5] Chusid, O.; Ein-Ely, Y.; Aurbach, D. *J. Power Sources* **1993**, *43*, 47.

[6] Gaberscek, M.; Jamnik, J.; Pejovnik, S. *J. Elecrochem. Soc.* **1993**, *140*, 308.

[7] Peled, E.; Menachem, C.; Bar-Tow, D.; Melman, A. *J. Electrochem. Soc.* **1996**, *143*, L4.

[8] Xing, W.; Dahn, J. R. *J. Electrochem. Soc.* **1997**, *144*, 1195.

[9] Matsumura, Y.; Wang, S.; Mondori, J. *J. Electrochem. Soc.* **1995**, *142*, 2914.

[10] Dey, A. N.; Sullivan, B. P. *J. Electrochem. Soc.* **1970**, *117*, 222.

[11] Arakawa, M.; Yamaki, J. *J. Electrochem. Soc.* **1987**, *134*, 273.

[12] Tarascon, J. M.; Guyomard, D. *Electrochemica Acta* **1993**, *38*, 1221.

[13] Fong, R.; Sacken, U. von; Dahn, J. R. *J. Electrochem. Soc.* **1990**, *137*, 2009.

[14] Wang, C. S.; Wu, G. T.; Li, W. Z. *J. Power Sources* **1998**, *76*, 1.

[15] Pacault, A. "*Chem. & Phys. of Carbon*", Vol. 7, ed. P. L. Walker, Jr., Marcel Dekker, New York, 1971, 107.

[16] Doh, C. H.; Moon, S. I.; Kim, W. S.; Yun, M. S. *Bull. Kor. Chem. Soc.* **1996**, *17*, 861.

[17] Mabuchi, A.; Tokumitsu, K.; Fujomoto, H.; Kasuh, T. *J. Electrochem. Soc.* **1995**, *142*, 1041.

[18] Doh, C. H.; Moon, S. I.; Yum, D. H.; Yun, M. S. Meeting Abstracts of The 195th Meeting of The Electrochemical Society, Seattle, U.S.A., 1999, 63.

[19] Iriyama, T.; Hashimoto, T.; Yamazaki, S.; Kawakami, F.; Shiroki, H.; Yamabe, T. *J. Power Sources* **1995**, *56*, 205.

[20] Watanabe, M.; Komaba, S.; Osaka, T.; Kikuyama, S.; Yuasa, K. *Electrochemica Acta* **1998**, *43*, 3127.

[21] Yamabe, T.; Tanaka, K.; Ago, H.; Yoshizawa, K.; Yata, S. *Syn. Met.* **1997**, *86*, 2411.

[22] Jean, M.; Desnoyer, C.; Tranchant, A.; Messia, R. *J. Electrochem. Soc.* **1995**, *142*, 2122.